An Evaluation of Three Different Techniques for Melt Impregnation of Glass Fiber Bundles With Polyamide 12

Willem Van De Steene,[1] **Jan Verstockt**,[1] **Joris Degrieck**,[2] **Kim Ragaert**,[1] **Ludwig Cardon**[1]
[1]*Department of Materials, Textiles and Chemical Engineering, Centre for Polymer and Material Technologies, Ghent University, Tech Lane Ghent Science Park – Campus A, Technologiepark 915, Zwijnaarde 9052, Belgium*
[2]*Department of Materials, Textiles and Chemical Engineering, Mechanics of Materials and Structures, Ghent University, Tech Lane Ghent Science Park – Campus A, Technologiepark 903, Zwijnaarde 9052, Belgium*

In this research, three different techniques for melt impregnation of glass fiber bundles with polyamide 12 are assessed with the aim of creating a high strength and modulus material suitable for extrusion based additive manufacturing. Impregnation quality of three production techniques: "Pultrusion", "PassivePin", and "ActivePin" were analyzed using three methods: matrix material mass fraction (M_m) determination, scanning electron microscopy of composite fracture surfaces and optical microscopy of polished composite cross sections. Pultrusion material has an overall poor impregnation degree (D_i) and fiber distribution and dispersion, the specimens lack mechanical strength and show fiber pull-out due to the excessive voids in the matrix. The PassivePin material has a significantly higher D_i and a better fiber distribution, which results in less voids in the matrix and limited fiber pull-out. Finally, the ActivePin material scores significantly higher in D_i and shows an excellent fiber distribution. As a consequence, very limited voids are observed and an even fracture surface without fiber pull-out is obtained. It is concluded that the ActivePin technique would be a great choice for application in an extrusion-based AM process, this method could allow for production of high strength and stiffness objects. POLYM. ENG. SCI., 58:601–608, 2018.

INTRODUCTION

Additive manufacturing (AM) and more specifically extrusion based fused deposition modeling is an interesting technique that has taken a giant leap forward during the last quarter-century. Despite its popularity, the lack of materials adapted to the processing methods has been an inhibitor for the advancement of the technology, especially to create high strength and high modulus objects.

A first solution consisted in adding short reinforcement fibers to thermoplastic materials for higher strength, stiffness and thermal stability and was researched by Gray et al. [1] Ning et al. [2], Tekinalp et al. [3], Karsli et al. [4], Zhong et al. [5], Fu et al. [6], Bijsterbosch et al. [7], and Compton et al. [8]. Nonetheless, the addition of short fibers to those materials tends to increase its brittleness [6, 7, 9]. The addition of continuous fibers to thermoplastic materials could be an advanced solution to enhance the mechanical properties of these short fiber reinforced thermoplastics [10, 11]. However, due to the high melt viscosity of thermoplastic polymers, the impregnation of fiber bundles with thermoplastic polymers requires a thoughtful approach.

Multiple methods exist for impregnating continuous fiber bundles with a thermoplastic polymer. Two main techniques can be distinguished. On the one hand, there are those that impregnate fiber bundles by submersion or pultrusion in a liquid matrix medium that is, a polymer melt, a solution or a monomer precursor. On the other hand, there are impregnation techniques that start from a solid matrix that is, thermoplastic polymer powders or spun fibers, followed by a mechanical infiltration process of the polymer into a fiber bundle and a sintering process to produce a pre-impregnated material, also referred to as "prepreg".

In 2015, a patent for an AM apparatus extruding thermoplastic prepregs was filed [12] by Mark et al. This technique strongly resembles automated fiber placement (AFP) and automated tape laying (ATL), where continuous fiber prepregs are deposited onto a mold [13, 14], but Mark's apparatus typically creates objects on a much smaller scale. Van Der Klift et al. [15] and Melenka et al. [16] performed mechanical tests on respectively continuous carbon fiber and aramid fiber filled polyamide tensile specimens created by this apparatus and showed that the technique is able to produce high strength parts, when compared with regular thermoplastic AM parts. Yet, fiber volume fraction V_f was reported to be only 34.5% [15], which is rather low compared with typical volume fractions of ~55%–60% for unidirectional AFP and ATL produced material [17, 18] or ~60%–80% for traditionally compression molded unidirectional composites [19].

Matsuzaki et al. [20], Nanya et al. [21], and Tian et al. [22] proposed an extrusion-based process in which a continuous carbon fiber bundle is impregnated with polylactic acid (PLA) by pushing it through a melt chamber right before its deposition. Mori et al. [23] developed a similar process to coextrude carbon fibers in an acrylonitrile butadiene styrene (ABS) matrix. An overview of matrix and fiber materials and according fiber volume fractions V_f for mentioned research is given in Table 1.

The advantage of combining impregnation and deposition in one process, compared with two discrete processes in ATL, AFP and Mark's technique, is threefold. First, avoiding an extra production step has an economic advantage. In addition, melt impregnation will result in a more even temperature distribution over the cross section of the impregnated fiber bundle during the deposition process. This minimizes thermally induced

Correspondence to: L. Cardon; e-mail: ludwig.cardon@ugent.be
This publication is based on the paper and presentation by Willem Van De Steene on the International Conference on Polymers and Moulds Innovations 2016 and has been accepted as full paper into the Polymer Engineering & Science journal special Issue PMI.
Contract grant sponsor: Ghent University
DOI 10.1002/pen.24789
Published online in Wiley Online Library (wileyonlinelibrary.com).

stresses and deformations upon solidifying of the deposited composite material. Finally, only limited to no external heating (e.g., hot air or nitrogen) for melting is necessary, unlike processes that start from thermoplastic prepregs. This ensures minimal degradation at the surface of the pultruded composite.

This *in situ* melt impregnation approach requires a proper fiber bundle impregnation technique to be able to obtain a mechanically stiff and strong material [7, 24], with no or limited voids. For this reason, this research focusses on the impregnation of glass fiber bundles with a polyamide 12 (PA 12) using three different melt impregnation techniques.

A first experimental setup "Pultrusion" consists of pultruding a glass fiber bundle through a PA 12 melt chamber without further manipulations. In a second method "PassivePin", a pressure is generated between the fiber bundle and a spreader pin in the melt chamber. This pressure will be the driving force for a proper polymer melt impregnation. In order to avoid the occurrence of "dry contact" [25, 26] between the fiber bundle and a spreader pin, an active impregnation pin can be used. This active impregnation pin injects liquid polymer between the cylindrical contact surface of the spreader pin and the fiber bundle and is an advanced version of a design described by Unger in U.S. Patent 5,158,608 [27]. The effect of this feature on the impregnation quality is studied as a third technique "ActivePin".

This research will compare the impregnation quality of composite materials produced with the three described techniques. Therefore, matrix material mass fractions M_m of the three different composites will be determined as an estimator for degree of impregnation. Also, using scanning electron microscope (SEM) images of the impregnated fiber bundles' fractured cross sections will be made and a fracture analysis will be performed to gain insight into the relation of impregnation quality and observed failure mechanisms. Further, optical microscopy of polished composite cross sections will not only give the opportunity to study the degree of impregnation, but also gives information about dispersion and distribution of the fibers in the matrix. The results of different test methods will be compared and will be used to draw some important conclusions.

MATERIALS AND METHODS

Matrix and Reinforcement Material

Rilsamid AMN O TLD from Arkema, a PA 12, was used as the matrix material for the composite. The melt flow index was determined according to ISO 1133-1:2005 with a Zwick 4100 apparatus as 51.61 ± 2.04 g/10 min (confidence level 95%), measured at 230°C, 2.16 kg.

As fiber reinforcement material, a StarRov LFT^{plus} Direct Roving 853 continuous glass fiber from Johns Manville was used. Linear density was measured according to ISO 1889:2009 and has a value of $1{,}179.29 \pm 5.48$ tex (confidence level 95%).

Pressure Build-up with Spreader Pins

Thermoplastic polymers have a high melt viscosity compared with their thermoset counterparts. For this reason, fiber impregnation with thermoplastics often occurs at high temperature and under high pressure (e.g., compression molding). With the aid of spreader pins in the melt chamber though, a local high pressure can be generated in a low-pressure environment, which eliminates the need for high strength and heavy tooling.

TABLE 1. overview of recently researched continuous fiber AM materials and their fiber volume fractions.

Research	Fiber material	Matrix material	V_f (%)
Mark	carbon	polyamide	34.5[a]
Matsuzaki	carbon	PLA	6.6
Matsuzaki	jute	PLA	6.2
Nanya	carbon	PLA	34
Tian et al.	carbon	PLA	27
Mori	carbon	ABS	0.2–1.6

[a]Preliminary result, further research needed on maximum volume fractions for different types of fibers.

By wrapping a tensioned fiber bundle (dashed line on Fig. 1) over a cylindrical surface, over a certain contact angle θ, a normal force is generated between both surfaces, which will result in a pressure p_x at point X between the fiber bundle and the surface. When the fiber bundle is pulled over the spreader pin, a continuous flow of polymer will be drawn between fiber bundle and surface. The pressure build-up will induce an outward radial flow of molten polymer through the fiber bundle. For low fiber velocities, the pressure (1), (2) can be approximated by tension force T_1, drag forces $T_{d,1}$ and $T_{d,2}$, the dynamic friction coefficient μ_d of the fiber bundle on the cylindrical surface (wet or dry contact), radius r of the impregnation pin and fiber bundle contact width w [28]. The necessary pulling force T_2 for a constant pultrusion velocity v, can be calculated as (3). As an extra advantage, the process with spreader pins induces high shear in the melt [11, 26, 29], which reduces the viscosity of the polymer, since it has shear-thinning characteristics. This effect will also promote impregnation [29, 30].

$$T_x = \left(T_1 + T_{d,1}\right) e^{\theta_x \cdot \mu_d} \tag{1}$$

$$p_x = \frac{T_x}{r \cdot w} \tag{2}$$

$$T_2 = \left(T_1 + T_{d,1}\right) e^{\theta \cdot \mu_d} + T_{d,2} \tag{3}$$

A common problem reported in fiber bundle impregnation literature is the forming of a dry contact zone between fiber and spreader pin for large wrapping angles. This phenomenon can be explained as follows: due to the polymer melt drag flow around the fiber bundle, a thin polymer film is formed between the fiber bundle and the pin. The pressure will cause the melt film to migrate through the fiber bundle. For high pressures or long wrapping angles, this polymer film could get depleted before the end of the contact zone, so there will be no extra gain in impregnation quality when exceeding a certain contact angle. Therefore, it can be useful to create a cascade of different spreader pins that have lower individual contact angles.

An alternative for the passive spreader pin is an active impregnation pin, in which liquid polymer is continuously added in the convex shaped contact region through small radial holes (Fig. 2) to prevent dry contact between pin and fiber. This design is an in-house developed, advanced version of a design described in US Patent 5,158,608 [27]. The developed device will be discussed in "Melt impregnation devices" Section.

DOI 10.1002/pen

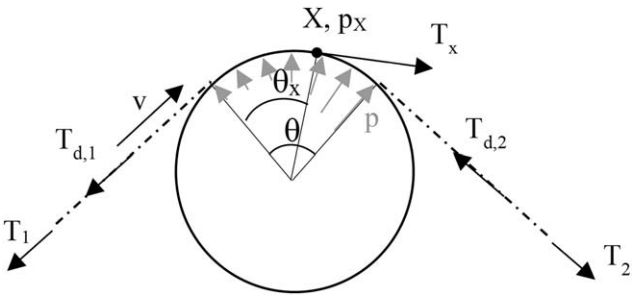

FIG. 1. Fiber bundle (dashed line) wrapped around spreader pin.

Melt Impregnation Devices

Within this research, two melt impregnation devices suitable for processing PA 12 and glass fiber, were developed. A regular pultrusion melt impregnation device as shown in Fig. 3, was developed to create the Pultrusion material. The glass fiber bundle (dashed line on Fig. 3) is pulled through an entrance die (No. 1 on Fig. 3), through the melt chamber (No. 3 on Fig. 3) and through the exit die (No. 4 on Fig. 3). Molten polymer material is added from No. 2 on Fig. 3.

Second, a spreader pin melt impregnation device to create the PassivePin and ActivePin material was developed (Fig. 2). The glass fiber bundle (presented by a dashed line on Fig. 2) is pulled through the entrance die (No. 0 on Fig. 2), which prevents the polymer melt from flowing out of the melt chamber, since the chamber is fully filled with molten polymer. After being guided by pin No. 1 (Fig. 2) to prevent the fiber bundle from contact with the die mold wall, the fiber bundle can be guided between or over spreader pins No. 2 and 3 (Fig. 2), which are mounted on an indexable drum to be able to adjust the contact angle. In Fig. 2, the drum is indexed so that there is no contact with the fiber bundle. Following is an active impregnation pin No. 4 (Fig. 2a) which can be rotated to position its seven injection holes away from the fiber bundle to become a passive spreader pin. The holes have a diameter of 1.5 mm and are located at every 30° of the cross section. Through these holes, polymer can be injected. Further, the fiber bundle passes through spreader pins No. 5 and 6 (Fig. 2), which have the same functionality as pins No. 2 and 3 (Fig. 2). Finally, the bundle is guided over pin No. 7 (Fig. 2) before exiting the spreader pin device through the pultrusion die (No. 8 on Fig. 2), which, in this case, has a diameter of 1.1 mm and wipes the excess PA 12 off the pultruded strand.

Composite Production Process

An in house developed extruder with screw diameter 10 mm, a compression ratio of 1.8 and an l/d ratio of 10 was connected to both impregnation devices and is able to inject molten polymer in the melt chamber of both melt impregnation devices. The rotational speed of the extruder screw was set at 10 rpm and the barrel was set at 90°C in the feed zone, increasing to 220°C in the metering zone. The temperature of the impregnation devices' housing was set at 220°C. Velocity of the glass fiber pultrusion was set at 600 mm/min. Three tests were conducted, starting from a virgin glass fiber bundle. Composite "Pultrusion" was produced in the regular pultrusion melt

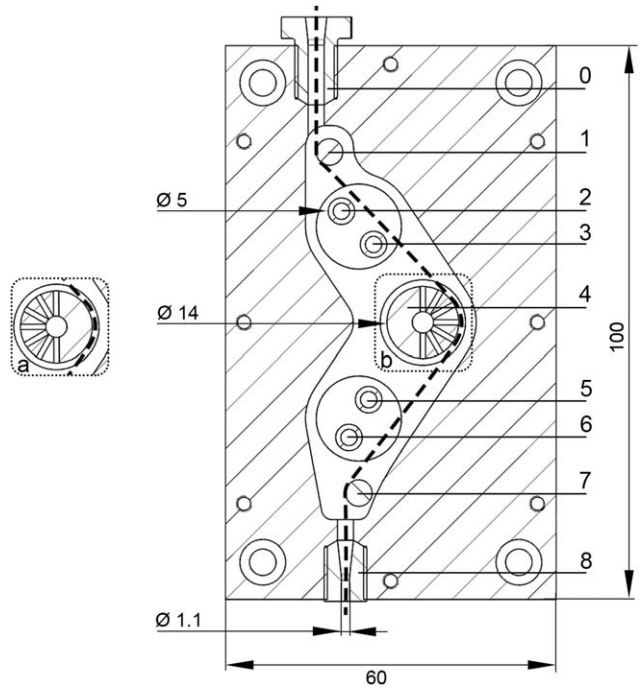

FIG. 2. Spreader pin melt impregnation device, (a) PassivePin, (b) ActivePin, dimensions in mm.

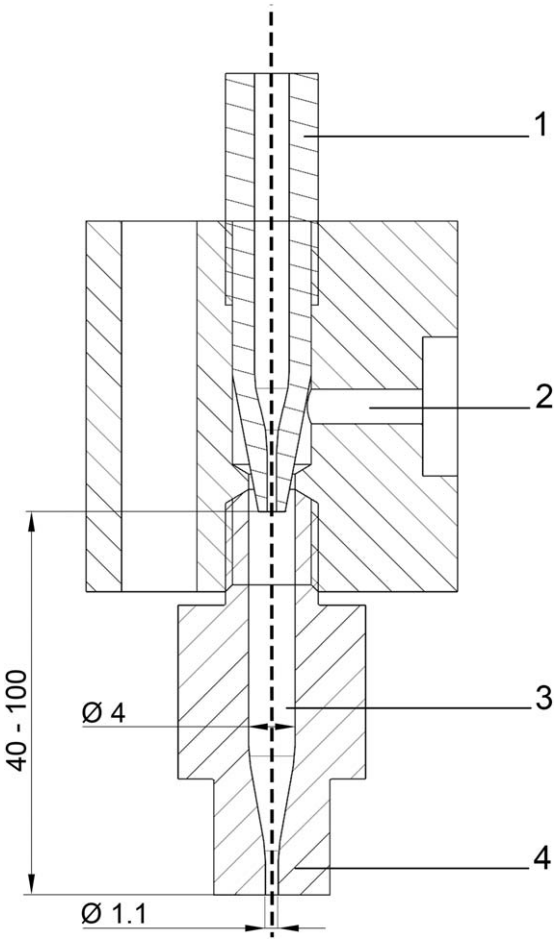

FIG. 3. Regular pultrusion melt impregnation device, dimensions in mm.

impregnation device as seen on Fig. 3. "PassivePin" was produced in the spreader pin melt impregnation device as seen on Fig. 2a with spreader pins Nos. 2–3 and 5–6 disabled and with the polymer channels of the active impregnation pin faced away from the fiber bundle. Composite "ActivePin" was produced on the spreader pin melt impregnation device with spreader pins Nos. 2–3 and 5–6 disabled and with the polymer channels of the active impregnation pin faced to the glass fiber bundle (Fig. 2b), which allows them to extrude polymer between the convex surface of the impregnation pin and the fiber bundle. It should be noted that the path length of the fiber bundle inside the regular Pultrusion device was chosen just as long as the path length of the fiber bundle in PassivePin and ActivePin configurations of the spreader pin device. All other parameters such as temperatures, pultrusion die diameter, fiber bundle tensions, pressures, and so on. were kept constant. This also implies that possible excess polymer leakage through the pultrusion die would be equal in all production processes.

Quantifying Impregnation Quality by Matrix Mass Fraction Determination

The mass fraction of the matrix material M_m will provide a quantification of the impregnation quality of the pultruded composite; a better impregnation will result in a larger M_m, providing there was no fiber fraction lost during the pultrusion process and there was no polymer leakage through the pultrusion die. The maximal obtainable matrix mass fraction $M_{m,max}$ of the composite material can be calculated from the linear density of the fiber bundle L, density of matrix ρ_m and fiber material ρ_f, composite mass m_c, matrix mass m_m, fiber mass m_f, matrix volume fraction V_m and fiber volume fraction V_f and inside diameter of the pultrusion die d_d (4). For this setup, a theoretical $M_{m,max}$ of 0.291 g/g was found, which is equivalent to a V_f of 49.3%. The degree of impregnation D_i can be calculated by (5), on the condition there is no polymer leakage between the pultrusion die wall and the wetted fiber bundle. Since there is a possibility of polymer leakage in this setup, no formal conclusions are drawn concerning the absolute degree of impregnation. In this research, the obtained data are used to relatively compare three production methods. An absolute determination of degree of impregnation can be done using micro tomography or by calculating the mean value of the void to void + matrix area ratio, measured in different cross sections of a specimen.

$$\begin{cases} V_f = \dfrac{4 \cdot L}{\pi \cdot \rho_f \cdot d_d^2} \\ V_m = 1 - V_f \\ M_{m,max} = \dfrac{V_m \cdot \rho_m}{V_m \cdot \rho_m + V_f \cdot \rho_f} \end{cases} \tag{4}$$

$$D_i = \frac{M_m}{M_{m,max}} \tag{5}$$

$$M_m = \frac{m_m}{m_c} = \frac{m_c - m_f}{m_c} \tag{6}$$

Before material sampling, the first and last 500 mm of the pultruded strands were discarded. In order to get a statistically significant result for the M_m values, for each material sample, 20 composite specimens with a length of 100 ± 1 mm were collected with a distance of 50 ± 1 mm between subsequent specimens on the pultruded strand. Those shorter parts were used during the optical and SEM microscopy analyses. The distance between specimens was kept low on purpose to reduce the possible effect of fiber mass loss due to fiber failure in the pultrusion die. This phenomenon could be falsely interpreted as an increase in M_m, thus would wrongly overestimate impregnation quality. To be able to exclude fiber failure in the melt chamber during production of the three samples, the content of the melt chamber was incinerated after production. In the rare case that fibers were found in the residual fraction, all specimens of that specific production run were discarded and produced anew.

The specimens of the produced composites were dried at 80°C for 8 h and were weighed using a Precisa XR 205SM-DR apparatus. Then, the specimens were incinerated for 15 minutes at a temperature of 550°C in a Nabertherm P300 oven. Subsequently, the residual mass of the specimens was weighed using previously mentioned Precisa apparatus and corresponds to the fiber mass m_f. The mass loss during incineration corresponds with m_m. M_m was calculated by formula (6), with m_c the initial mass of the composite specimen before incineration. Due to the relatively low density of entrapped gasses in the samples compared with the matrix and fiber density, the mass fraction of the voids M_v was neglected.

To check whether there is a statistically significant influence of the three production techniques on the impregnation quality and thus on M_m, a one way ANOVA test was conducted to compare the M_m of composites Pultrusion (produced using a regular pultrusion process), PassivePin (produced with passive spreader pin) and ActivePin (produced with active impregnation pin) at a 95% confidence level.

Visual Evaluation of Impregnation Quality by Fracture Analysis

A visual evaluation of the fiber bundles' impregnation quality was done using SEM of fractured composite specimens. To this end, specimens were fully submersed in liquid nitrogen for 60 s and broken perpendicular to the fiber direction immediately afterwards. It was impossible to obtain fully brittle fracture surfaces due to the ductile behavior of the PA 12 matrix material, even at extremely low temperatures (boiling point of liquid nitrogen is −196°C).

Before imaging, the specimens were gold sputtered during 60 s with a current of 25 mA. An accelerating voltage of 5 kV, working distances between 11 and 13 mm and magnifications of 250 were used on a Jeol JSM-7600F apparatus in secondary electron imaging mode for visualizing the fracture surface.

Inspecting Impregnation Quality Using Optical Microscopy

The composite specimens of the three different production methods were embedded using a cold curing epoxy Epofix from Struers. Specimens were ground and polished to reveal the cross section of the impregnated bundle. The cross sections of three different composites were visualized using a Keyence VHX-500F Digital optical microscope. Optical microscopy at magnifications of 200 allowed for visualizing features such as fiber distribution and dispersion, location of the voids, etc.

 DOI 10.1002/pen

TABLE 2. Statistical analysis of matrix material mass fraction.

Composite material	n #	Mean M_m (g/g)	SD (g/g)	Mean D_i (%)	SD (%)
Pultrusion	20	0.217	0.0130	74.5	4.46
PassivePin	20	0.269	0.0123	92.2	4.21
ActivePin	20	0.285	0.0123	98.0	4.21

RESULTS AND DISCUSSION

Matrix Mass Fraction Determination Results

Table 2 shows the mean values and standard deviations of the M_m for the three produced composites. A statistically significant difference in M_m was measured for Pultrusion, PassivePin and ActivePin as determined by one-way ANOVA ($F[2,57] = 163.46$, $p = 0.000$). It is concluded that the use of a passive ($M_m = 0.269 \pm 0.0241$ g/g) or an active impregnation pin ($M_m = 0.285 \pm 0.0241$ g/g) drastically improves the M_m compared with the pultrusion production technique ($M_m = 0.217 \pm 0.0255$ g/g). The use of an active impregnation pin rather than a passive spreader pin further improves M_m and related impregnation quality.

A bar chart with the mean M_m of three composites can be found in Fig. 4. The theoretical maximum mass fraction $M_{m,max}$ for the described machine configuration ("Melt impregnation devices" and "Composite production process" Section) was calculated by *Eq. 4*, has a value of 0.291 g/g and is displayed as a horizontal line on Fig. 4. The three mean M_m values are below this maximum value, some ActivePin M_m measurements exceeded the theoretical maximum value. Two possible explanations for this phenomenon can be found: the 1 mg error of the used Precisa balance translates in an error of $\pm$ 2% in impregnation degree, another possibility is that there was a limited amount of polymer leaking between die walls and impregnated fiber bundle. It is concluded that mass fraction measurements are a good way of showing relative differences in impregnation quality; however, they should be combined with visual tests to draw conclusions on the absolute impregnation degree and fiber dispersion in the matrix.

Scanning Electron Microscopy Results

Fracture surfaces of the composite material samples Pultrusion (Fig. 5), PassivePin (Fig. 6), and ActivePin (Fig. 7) were visualized with SEM. Comparison of the samples shows important differences in fracture surface topographies.

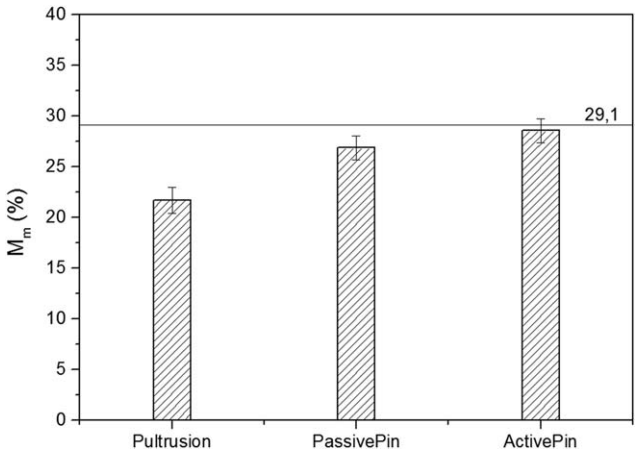

FIG. 4. Mean matrix material mass fractions for three production techniques (1 SD error bars).

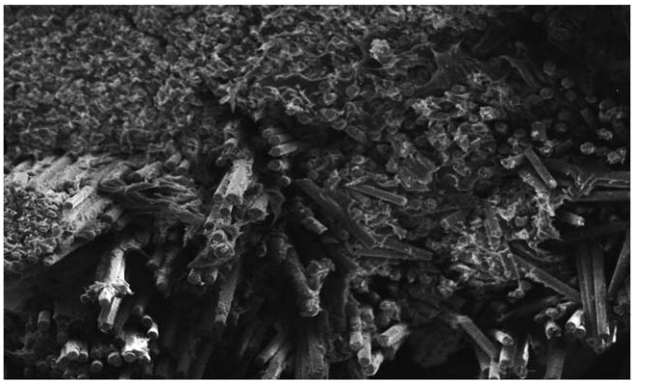

FIG. 5. SEM image of a fractured Pultrusion specimen (×250).

A micrograph of the sample Pultrusion can be seen on Fig. 5. Peaks of loose fibers and locations of fiber-pull out can be observed. This phenomenon is caused by axially oriented voids inside the matrix that form stress concentrators and mainly reduce shear moduli $G_{1,2}$ and $G_{1,3}$ [24]. These axially oriented voids situated between adjacent fibers initiate plastic shear while fracturing a specimen during specimen preparation. Tensile or compression forces on fibers close to voids will create high fiber stresses, since the matrix's ability for stress distribution is limited there. When individual fiber tensile strength is reached, the fiber will break; stresses will be redistributed in the specimen, which will eventually lead to a cascade effect of failing fibers. The fractured fibers will be pulled out of the matrix and cause the described topography. Further, locations without impregnation can be remarked. This result is in line with the conclusions made in the M_m analysis.

It can be seen that specimen PassivePin (Fig. 6) has a fracture surface with peaks of loose fibers (Nos. 1–3 on Fig. 6) and indentations where fibers were pulled out during specimen fracturing (Nos. 4 and 5 on Fig. 6). This effect is caused by the same phenomenon which occurred also in the Pultrusion specimen.

Also, several dark spots can be noticed, spread on the fracture surface, which confirms the voids between adjacent fibers.

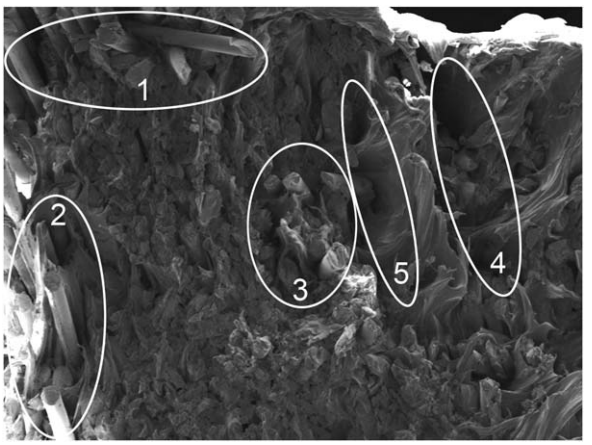

FIG. 6. SEM image of a fractured PassivePin specimen (×250).

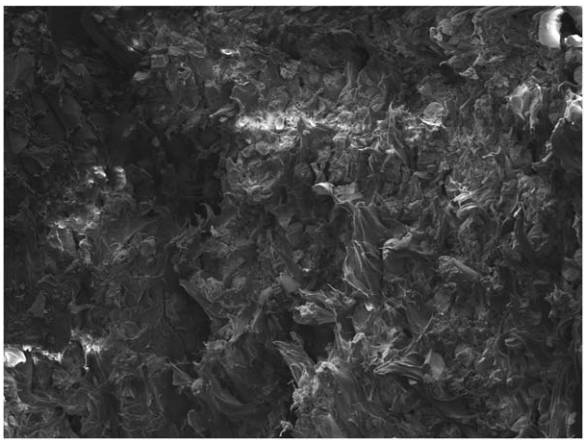

FIG. 7. SEM image of a fractured ActivePin specimen (×250).

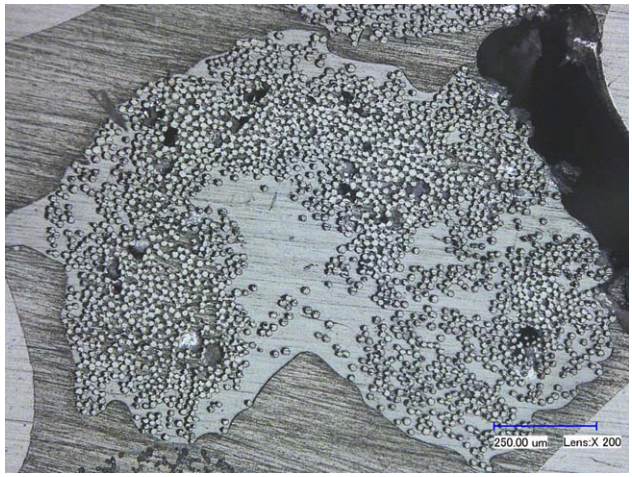

FIG. 9. Optical microscopy image of a PassivePin specimen. [Color figure can be viewed at wileyonlinelibrary.com]

It is concluded that the passive impregnation pins fail to fully impregnate the fiber bundle.

The fracture surface of sample ActivePin (Fig. 7) shows a more even topography since there was less to no axial voids that can propagate shear cracking in planes parallel to the main fiber direction. This reduces fiber pull-out and results in a smoother fracture surface. Fibers remain firmly embedded in the matrix material after fracture.

Note that for the three materials' surfaces, plastically deformed parts of the PA 12 matrix can be seen, which implies that the used specimen preparation method fails to cause a fully brittle fracture.

Optical Microscopy Results

A micrograph of composite material produced using the regular pultrusion method can be seen in Fig. 8. After the pultrusion process, the original tape like fiber bundle was still as it was supplied, but was folded round a core of recognizable polymer (No. 1 on Fig. 8). The poor fiber dispersion is attributed to the lack of manipulation and spreading during pultrusion of the slightly coagulated fibers. This coagulation is a consequence of the coating or "sizing" which is applied to fiber bundles during their manufacturing process. Within the fiber bundle itself, poor to moderate impregnation was observed. At No. 2 on Fig. 8, epoxy material from the embedding process was observed in the fiber bundle, which means it was a void area before embedding. It is concluded that despite the moderate M_m of the composite, the inferior fiber distribution and dispersion renders the composite unsuitable for high mechanical property applications.

When comparing composites produced using Pultrusion (Fig. 8) and PassivePin (Fig. 9), a clear difference in fiber dispersion and degree of impregnation can be seen. A passive spreader pin is able to disintegrate the coagulated fiber bundles, enhance the fiber's permeability and impregnate them. Nonetheless, some zones within the fibers were not impregnated with PA 12 during production; some clear voids can be seen in the micrograph. It is concluded that by using a passive impregnation pin, a better quality of impregnation can be achieved, compared with a standard pultrusion process.

Studying the ActivePin micrograph (Fig. 10) it can be seen that both fiber dispersion and distribution is reasonably good. Except for some smaller zones where voids occurred, the degree of impregnation is sufficient. It is concluded that the ActivePin

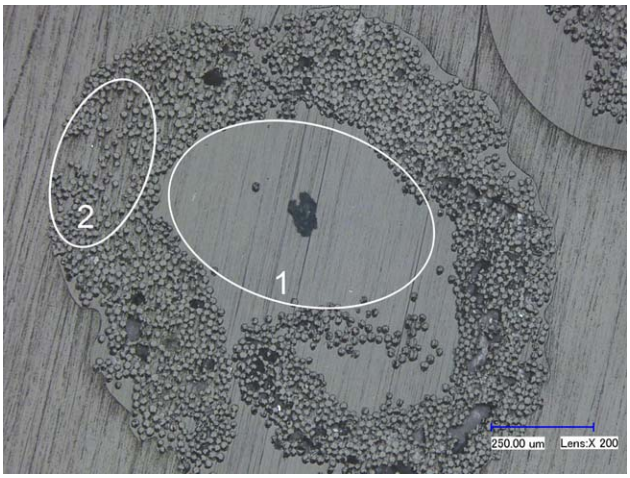

FIG. 8. Optical microscopy image of a Pultrusion specimen. [Color figure can be viewed at wileyonlinelibrary.com]

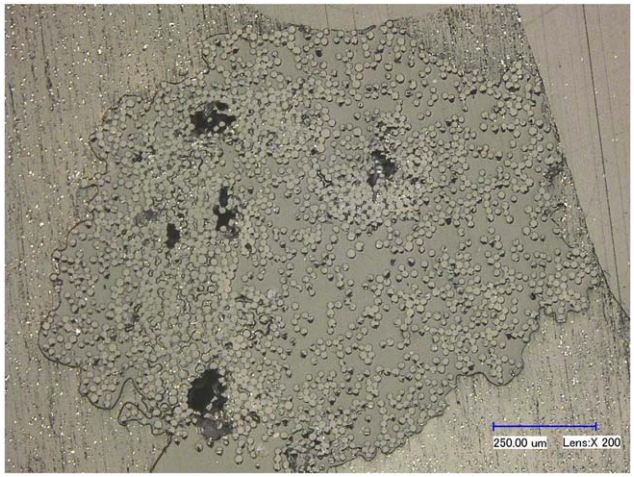

FIG. 10. Optical microscopy image of an ActivePin specimen. [Color figure can be viewed at wileyonlinelibrary.com]

DOI 10.1002/pen

outperforms the Pultrusion and PassivePin process when it comes to impregnation quality. This result is promising and indicates that high impregnation quality of PA 12 in glass fiber bundles can be achieved when using an optimized device.

CONCLUSIONS

This research assessed three techniques for melt impregnation of continuous glass fiber bundles with polyamide 12. Therefore, three materials were produced; one using the process "Pultrusion", one using "PassivePin" and a third using process "ActivePin".

Impregnation quality was analyzed using three methods: M_m determination, SEM of composite fracture surfaces and optical microscopy of polished composite cross sections.

Process Pultrusion resulted in a M_m of 0.217 ± 0.0255 g/g, PassivePin in 0.269 ± 0.0241 g/g and the ActivePin process in 0.285 ± 0.0241 g/g, where the theoretical maximum value for M_m was 0.291 g/g. It was concluded that both PassivePin and ActivePin perform significantly better than Pultrusion. Also, The ActivePin process significantly outperformed PassivePin. These results can be used as a relative comparison between the three production methods, but should be combined with optical results of composite cross sections to draw final conclusions about fiber distribution and dispersion.

SEM analysis of fractured composites specimens showed that voids were predominant in Pultrusion samples and fiber pull-out was initiated by the axially oriented voids. PassivePin only showed small voids and a limited amount of fiber pull-out at the void locations. In the fracture surface of ActivePin, fibers remained firmly embedded in the matrix;there was a good stress distribution during fracturing, which led to a smooth fracture topography.

During optical microscopy of the Pultrusion specimens, it was seen that the fiber bundle was wrapped around a polymer core and impregnation of the bundle was poor. In PassivePin specimens, the original shape of the fiber bundle was still recognizable but there was a better fiber distribution and dispersion compared with Pultrusion material. An excellent fiber dispersion of the fibers in the matrix and only a very limited of matrix voids were obtained with the ActivePin technique.

When comparing the analyses, it is clear that their conclusions are parallel. Pultrusion material has an overall poor impregnation degree, fiber distribution and dispersion, the specimens lack mechanical strength and show fiber pull-out due to the excessive voids in the matrix. PassivePin material has a higher impregnation degree and a better fiber distribution, which results in less voids in the matrix and limited fiber pull-out. Finally, the ActivePin material scores significantly higher in impregnation degree and shows an excellent fiber distribution. As a consequence, very limited voids are observed and an even fracture surface without fiber pull-out is obtained.

It is clear that the ActivePin technique would be a great choice for application in an extrusion-based AM process, this method could allow for production of high strength and stiffness objects.

In future research, it would be interesting to study whether the findings of this research can be extrapolated to other fiber and matrix materials. Further, it has to be researched whether the findings above correlate with the mechanical properties of AM manufactured continuous fiber reinforced material, and how these properties relate to conventionally produced thermoplastic composites.

ACKNOWLEDGMENTS

The authors wish to acknowledge Ghent University for funding this research. Furthermore, the authors thank the company Johns Manville for providing the glass fiber material.

NOMENCLATURE

ABS	Aminonitrile butadiene styrene
AFP	Automated fiber placement
AM	Additive manufacturing
ATL	Automated tape laying
d_d	Diameter of a pultrusion die
D_i	Degree of impregnation
FDM	Fused deposition modeling
$G_{1,2}$ and $G_{1,3}$	Shear moduli in a plane parallel to fiber direction in a uniaxially reinforced composite
L	Linear density of a fiber bundle
m_c	Mass of a composite material
m_f	Mass of a fiber material
m_m	Mass of a matrix material
M_f	Mass fraction of fibers in a composite
MFI	Melt flow index
M_m	Mass fraction of matrix in a composite
$M_{m,max}$	Maximum obtainable matrix mass fraction
M_v	Mass fraction of voids in a composite
μ_d	Dynamic friction coefficient
n	Amount of specimens
PA 12	Polyamide 12
PLA	Polylactic acid
p_x	Pressure at location x
R	Radius of a spreader/impregnation pin
ρ_f	Density of a fiber material
ρ_m	Density of a matrix material
SEM	Scanning electron microscopy
T_i	Tensile force number i
$T_{d,i}$	Drag force number i
T_x	Tensile force at location x
θ	Total contact angle
θ_x	Contact angle at location x
v	Pultrusion velocity
V_f	Volume fraction of fibers in a composite
V_m	Volume fraction of matrix in a composite
w	Fiber bundle contact width
X	Location x

REFERENCES

1. W. Gray, D.G. Baird, and J. Bøhn, *Polym. Compos.*, **19**, 4, (1998).
2. F. Ning, W. Cong, Y. Hu, and H. Wang, *J. Compos. Mater.*, **80**, 369 (2016).
3. H.L. Tekinalp, V. Kunc, G.M. Velez-Garcia, C.E. Duty, L.J. Love, A.K. Naskar, C.A. Blue, and S. Ozcan, *Compos. Sci. Technol.*, **105**, 144 (2014).
4. N.G. Karsli, and A. Aytac, *Compos. Part B: Eng.*, **51**, 270 (2013).

5. W. Zhong, F. Li, Z. Zhang, L. Song, and Z. Li, *Mater. Sci. Eng.*, **A301**, 301 (2001).
6. S.-Y. Fu, B. Lauke, E. Mäder, C.-Y. Yue, and X. Hu, *Compos. Part A Appl. Sci. Manuf.*, **31**, 1117 (2000).
7. H. Bijsterbosch and R.J. Gaymans, *Polym. Compos.*, **16**, 363 (1995).
8. B.G. Compton and J.A. Lewis, *Adv. Mater.*, **26**, 6043 (2014).
9. S. Kumar and J. Kruth, *Mat. Des.*, **31**, 850 (2009).
10. T.M. Llewellyn-Jones, B.W. Drinkwater, and R.S. Trask, *Smart Mater. Struct.*, **25**, 02LT01 (2016).
11. R. Marissen, L.T. Van Der Drift, and J. Sterk, *Compos. Sci. Technol.*, **60**, 2029 (2000).
12. G.M. Mark, U.S. Patent 2015/0165691 A1 (2015).
13. D.H.J.A. Lukaszewicz, C. Ward, and K.D. Potter, *Compos. Part B Eng.*, **43**, 997 (2012).
14. Z. Qureshi, T. Swait, R. Scaife, and H.M. El-Dessouky, *Compos. Part B Eng.*, **66**, 255 (2014).
15. F. Van Der Klift, Y. Koga, A. Todoroki, M. Ueda, and Y. Hirano, *Open J. Compos. Mater.*, **6**, 18 (2016).
16. G.W. Melenka, B.K.O. Cheung, J.S. Schofield, M.R. Dawson, and J.P. Carey, *Compos. Struct.*, **153**, 866 (2016).
17. A.J. Comer, D. Ray, W.O. Obande, D. Jones, J. Lyons, I. Rosca, R.M. O' Higgins, and M.A. McCarthy, *Compos. Part A: Appl. Sci. Manuf.*, **69**, 10 (2015).
18. C.M. Stokes-Griffin, and P. Compston, *Opt. Lasers Eng.*, **72**, 1 (2015).
19. D.M. Corbridge, L.T. Harper, D.S.A. De Focatiis, and N.A. Warrior, *Compos. Part A: Appl. Sci. Manuf.*, **95**, 87 (2017).
20. R. Matsuzaki, M. Ueda, M. Namiki, T.-K. Jeong, H. Asahara, K. Horiguchi, T. Nakamura, A. Todoroki, and Y. Hirano, *Sci. Rep.*, **6**, (2016).
21. N. Li, Y. Li, and S. Liu, *J. Mater. Process. Technol.*, **238**, 218 (2016).
22. X. Tian, T. Liu, C. Yang, Q. Wang, and D. Li, *Compos. Part A: Appl. Sci. Manuf.*, **88**, 198 (2016).
23. K.-I. Mori, T. Maeno, and Y. Nakagawa, *Procedia Eng.*, **81**, 1595 (2014).
24. H. Huang and R. Talreja, *Compos. Sci. Technol.*, **65**, 1964 (2005).
25. R.J. Gaymans, and E. Wevers, *Compos. Part A: Appl. Sci. Manuf.*, **29**, 663 (1998).
26. P.J. Bates, J. Kendall, D. Taylor, and M. Cunningham, *Compos. Sci. Technol.*, **62**, 379 (2002).
27. M. Unger, U.S. Patent 5,158,806 (1992).
28. P.J. Bates and J.M. Charrier, *Therm. Compos. Mat.*, **12**, 276 (1991).
29. R. Asthana and S.N. Tewari, *Compos. Manuf.*, **4**, 3 (1993).
30. C. Mayer, X. Wang, and M. Neitzel, *Compos. Part A Appl. Sci. Manuf.*, **29**, 783 (1998).

 DOI 10.1002/pen